

Tuning the Helicity of Self-Assembled Structure of a Sugar-Based Organogelator by the Proper Choice of Cooling Rate

Jiaxi Cui, Anhua Liu, Yan Guan, Jia Zheng, Zhihao Shen, and Xinhua Wan*

Beijing National Laboratory for Molecular Sciences, Key Laboratory of Polymer Chemistry and Physics of Ministry of Education, College of Chemistry and Molecular Engineering, Peking University, Beijing 100871, China

Received August 17, 2009. Revised Manuscript Received October 28, 2009

A novel sugar-appended low-molecular-mass gelator, 4'-butoxy-4-hydroxy-*p*-terphenyl- β -D-glucoside (BHTG), was synthesized. It formed thermally reversible gels in a variety of aqueous and organic solvents. Three-dimensional networks made up of helical ribbons were observed in the mixture of H₂O/1,4-dioxane (40/60 v/v). The handedness of the ribbons depended on the rate of gel formation. Fast-cooling process led to right-handed ribbons, while slow-cooling process led to left-handed ones. A combinatory analyses of microscopic, spectroscopic, and diffraction techniques revealed that BHTG formed a twisted interdigitated bilayer structure with a *d* spacing of 3.1 nm in gels through a kinetically controlled nucleation-growth process. There were two kinds of molecular orientations of BHTG in the nuclei, clockwise and anticlockwise, which dictated the growth of ribbons. One was metastable and formed first during the cooling process of gel formation. It was able to gradually transform into the more stable latter one with further decreasing temperature. Fast-cooling process did not leave enough time for the nuclei to evolve from metastable to stable state and the ribbons grown from them exhibited right-handedness. However, the metastable nuclei transformed into the stable one when cooled slowly and directed the molecules of BHTG to grow into left-handed aggregates.

Introduction

The self-assembly of small molecules and macromolecules into chiral aggregates by elegantly utilizing cooperative secondary forces is ubiquitous in nature.¹ Many key biological processes such as signaling, gene expression, and response to external stimulus rely on a delicate connection between molecular, macromolecular, and supramolecular chirality.² In recent years, robust passion has been put on the control over the chirality at various hierarchical levels.^{1c,3,4} Low-molecular-mass gelators (LMMGs) offer fascinating opportunities in the field due to their tendency to self-assemble into three-dimensional networks made up of chiral

fibrous aggregates spanning the whole system.⁵ Most LMMGs studied are chiral.⁶ Examples of which include steroid,^{7,8} amide- and urea-type,^{9,10} nucleobase derivatives,^{11,12} sugar amphiphiles,¹³⁻¹⁶ phospholipids, and so forth.^{5b,5d,17} Under the right circumstances, dictated by the built-in configurational chirality, the packings of these molecules are asymmetric and chiral aggregates such as

*To whom correspondence should be addressed. Phone: 86-10-62754187. Fax: 86-10-62751708. E-mail: xhwan@pku.edu.cn.

- (1) (a) Casper, D. L. D. *Biophys. J.* **1980**, *32*, 103–138. (b) Cornelissen, J. J. L. M.; Rowan, A. E.; Nolte, R. J. M.; Sommerdijk, N. A. J. M. *Chem. Rev.* **2001**, *101*, 4039–4070. (c) Rudick, J. G.; Percec, V. *Acc. Chem. Res.* **2008**, *41*, 1641–1652.
- (2) Fraenkel-Conrat, H.; Williams, R. C. *Proc. Natl. Acad. Sci. U.S.A.* **1955**, *41*, 690–698.
- (3) (a) Spector, M. S.; Selinger, J. V.; Schnur, J. M. In *Materials-Chirality*; Green, M. M., Nolte, R. J. M., Meijer, E. W., Eds.; John Wiley & Sons, Inc.: New York, 2003; Vol. 24, pp 281–372. (b) Hill, D. J.; Mio, M. J.; Prince, R. B.; Hughes, T. S.; Moore, J. S. *Chem. Rev.* **2001**, *101*, 3893–4012. (c) Nakano, T.; Okamoto, Y. *Chem. Rev.* **2001**, *101*, 4013–4038. (d) A series of reports about supramolecular chirality can be seen in *Top. Curr. Chem.* **2006**, *265*. (e) Bishop, R. *Acc. Chem. Res.* **2008**, *42*, 67–78. (f) Yashima, E.; Maeda, K.; Furusho, Y. *Acc. Chem. Res.* **2008**, *41*, 1166–1180.
- (4) (a) Engelkamp, H.; Middelbeek, S.; Nolte, R. J. M. *Science* **1999**, *284*, 785–788. (b) Orr, G. W.; Barbour, L. J.; Atwood, J. L. *Science* **1999**, *285*, 1049–1052. (c) Lehn, J. M. *Science* **2002**, *295*, 2400–2403.
- (5) (a) A series of reports about gelators can be seen in *Langmuir* **2009**, *25*, 8369–8840. (b) Terech, P.; Weiss, R. G. *Chem. Rev.* **1997**, *97*, 3133–3160. (c) van Esch, J. H.; Feringa, B. L. *Angew. Chem., Int. Ed.* **2000**, *39*, 2263–2266. (d) Estroff, L. A.; Hamilton, A. D. *Chem. Rev.* **2004**, *104*, 1201–1218. (e) Sugiyasu, K.; Fujita, N.; Shinkai, S. *J. Synth. Org. Chem. Jpn.* **2005**, *63*, 359–369.
- (6) Brizard, A.; Oda, R.; Huc, I. *Top. Curr. Chem.* **2005**, *256*, 167–218.
- (7) (a) Weiss, R. G. *Acc. Chem. Res.* **2006**, *39*, 489–497. (b) Žinić, M.; Vögtle, F.; Fages, F. *Top. Curr. Chem.* **2005**, *256*, 39–76. (d) Lu, L.; Cocker, T. M.; Bachman, R. E.; Weiss, R. G. *Langmuir* **2000**, *16*, 20–34.
- (8) (a) Jung, J. H.; Shinkai, S. *Top. Curr. Chem.* **2005**, *248*, 223–260. (b) Shinkai, S. *Tetrahedron* **1995**, *51*, 555–566. (c) Jung, J. H.; Shinkai, S.; Shimizu, T. *Chem. Mater.* **2003**, *15*, 2141–2145. (d) Sugiyasu, K.; Kawano, S.-i.; Fujita, N.; Shinkai, S. *Chem. Mater.* **2008**, *20*, 2863–2865.

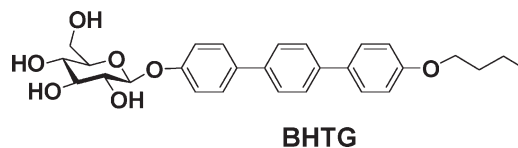
- (9) Fages, F.; Vögtle, F.; Žinić, M. *Top. Curr. Chem.* **2005**, *256*, 77–131.

- (10) (a) Shi, C.; Huang, Z.; Kilic, S.; Xu, J.; Enick, R. M.; Beckman, E. J.; Carr, A. J.; Melendez, R. E.; Hamilton, A. D. *Science* **1999**, *286*, 1540–1543. (b) Caplar, V.; Žinić, M.; Pozzo, J.-L.; Fages, F.; Mieden-Gundert, G.; Vögtle, F. *Eur. J. Org. Chem.* **2004**, *2004*, 4048–4059. (c) Bhuniya, S.; Park, S. M.; Kim, B. H. *Org. Lett.* **2005**, *7*, 1741–1744. (d) Suzuki, M.; Sato, T.; Shirai, H. *Chem. Commun.* **2006**, 377–379. (e) Dautel, O. J.; Robitzer, M.; Lere-Porte, J.-P.; Serein-Spirau, F.; Moreau, J. J. E. *J. Am. Chem. Soc.* **2006**, *128*, 16213–16223. (f) Palui, G.; Banerjee, A. J. *Phys. Chem. B* **2008**, *112*, 10107–10115. (g) Kim, J. H.; Seo, M.; Kim, Y. J.; Kim, S. Y. *Langmuir* **2009**, *25*, 1761–1766. (h) Yamanaka, M.; Fujii, H. *J. Org. Chem.* **2009**, *74*, 5390–5394.
- (11) Araki, K.; Yoshikawa, I. *Top. Curr. Chem.* **2005**, *256*, 133–165.
- (12) (a) Yanagawa, H.; Ogawa, Y.; Furuta, H.; Tsuno, K. *J. Am. Chem. Soc.* **1989**, *111*, 4567–4570. (b) Shimizu, T.; Iwaura, R.; Masuda, M.; Hanada, T.; Yase, K. *J. Am. Chem. Soc.* **2001**, *123*, 5947–5955. (c) Iwaura, R.; Yoshida, K.; Masuda, M.; Yase, K.; Shimizu, T. *Chem. Mater.* **2002**, *14*, 3047–3053. (d) Moreau, L.; Barthelemy, P.; El Maataoui, M.; Grinstaff, M. W. *J. Am. Chem. Soc.* **2004**, *126*, 7533–7539.
- (13) (a) Bhattacharya, S.; Acharya, S. N. G. *Langmuir* **1999**, *16*, 87–97. (b) Bhattacharya, S.; Acharya, S. N. G. *Chem. Mater.* **1999**, *11*, 3504–3511. (c) Srivastava, A.; Ghorai, S.; Bhattacharjya, A.; Bhattacharya, S. *J. Org. Chem.* **2005**, *70*, 6574–6582. (d) Bhattacharya, S.; Srivastava, A.; Pal, A. *Angew. Chem., Int. Ed.* **2006**, *45*, 2934–2937. (e) Pal, A.; Chhikara, B. S.; Govindaraj, A.; Bhattacharya, S.; Rao, C. N. R. *J. Mater. Chem.* **2008**, *18*, 2593–2600. (f) Samanta, S. K.; Pal, A.; Bhattacharya, S. *Langmuir* **2009**, *25*, 8567–8578.
- (14) (a) Yoza, K.; Amanokura, N.; Ono, Y.; Akao, T.; Shinmori, H.; Takeuchi, M.; Shinkai, S.; Reinhoudt, D. N. *Chem.—Eur. J.* **1999**, *2722–2729*. (b) Tamaru, S.; Nakamura, M.; Takeuchi, M.; Shinkai, S. *Org. Lett.* **2001**, *3*, 3631–3634. (c) Gronwald, O.; Shinkai, S. *Chem.—Eur. J.* **2001**, *20*, 4328–4334. (d) Jung, J. H.; Shinkai, S.; Shimizu, T. *Nano Lett.* **2002**, *2*, 17–20. (e) Jung, J. H.; John, G.; Yoshida, K.; Shimizu, T. *J. Am. Chem. Soc.* **2002**, *124*, 10674–10675. (f) Friggeri, A.; Gronwald, O.; van Bommel, K. J. C.; Shinkai, S.; Reinhoudt, D. N. *J. Am. Chem. Soc.* **2002**, *124*, 10754–10758. (g) Karinaga, R.; Jeong, Y.; Shinkai, S.; Kaneko, K.; Sakurai, K. *Langmuir* **2005**, *21*, 9398–9401.
- (15) (a) Cui, J.; Zheng, J.; Qiao, W.; Wan, X. *J. Colloid Interface Sci.* **2008**, *326*, 267–274. (b) Zheng, J.; Qiao, W.; Wan, X.; Gao, J. P.; Wang, Z. *Y. Chem. Mater.* **2008**, *20*, 6163–6168. (c) Cui, J.; Shen, Z.; Wan, X. *Langmuir* **2009**, ASAP, doi: 10.1021/la9021382.
- (16) Ghosh, R.; Chakraborty, A.; Maiti, D. K.; Puranik, V. G. *Org. Lett.* **2006**, *8*, 1061–1064.

twisting fibrils and helical ribbons are therefore generated.⁶ In general, the handedness of a chiral superstructure reflects the underlying chirality of the subclass building blocks.¹⁸ One enantiomer gives a right-handed aggregate, while the other gives a left-handed one.¹⁹ However, several conflicting examples have been reported recently. Thomas and co-workers found the simultaneous formation of right- and left-handed helical ribbons by an enantiomerically pure phosphonate analogue of 1,2-bis(10,12-tricosadiynoyl)-*sn*-glycero-3-phosphocholine (DC(8,9)PC) and the related compounds.²⁰ Zastavker et al. obtained similar results in a variety of multicomponent enantiomerically pure systems containing a bile salt or a nonionic detergent, a phosphatidylcholine or a fatty acid, and a steroid analogue of cholesterol.²¹ Moreover, Ho, Hsu, and their co-workers observed the dependence of helical twisting power on the length of achiral alkyl tail in a series of sugar-appended Schiff base rod-coil amphiphiles.²² These interesting findings demonstrate, on the one hand, the complexity in the generation, transfer, and expression of chirality during the formation of hierarchical supramolecular structures. It enables us, on the other hand, to tune the handedness of the chiral aggregates without changing the chemistry of the building blocks.

A gel is usually prepared by first dissolving LMMG in a certain solvent at high temperature and then cooling the hot solution to a lower temperature.²³ In this sense, thermal control might represent one of the most convenient methods to tune the substructures of the gel from LMMG. Indeed, Weiss et al. noticed a correlation between the cooling rate and the length and thickness of the fibers from anthraquinone-appended steroid-based gelators.²⁴ Shinkai and co-workers found that the sign inversion of circular dichroism (CD) effects of the gels from some azobenzene-linked cholesterol derivatives depended on the rate of network formation.²⁵ Especially, in a chiral optical molecular switch system reported by van Esch and Feringa,²⁶ reversible transcription of supramolecular chirality to molecular chirality with nearly complete stereoselectivity was achieved through locking metastable chiral assemblies in gel by a combination of thermal and light control. The molecular switch had open and closed forms. Irradiation of the open form in the gel phase yielded metastable assembly of closed form, which was regulated to be a stable state. The stable state of the closed form produced a metastable state of the open form by irradiation. Thus, tetra-state cycle can be carried out conveniently by regulating the metastable state of the open form to be a stable one. Sugar-appended gelators are a large family of LMMGs displaying remarkable diversity in gelation ability and supramolecular structures.^{13–15} The preparation and structures of hollow glycolipid

Chart 1. Chemical Structure of BHTG



nanotubes and their precursors, helical fibrous ribbons, have been systematically investigated.²⁷ However, no work on the thermal control of supramolecular chirality of sugar-appended gelator has been known.

In this study, we report the synthesis, gelling behavior, and cooling rate dependence of supramolecular chirality of a novel sugar-based gelator, 4'-butoxy-4-hydroxy-*p*-terphenyl- β -D-glucoside (BHTG), in a mixture of H₂O/1,4-dioxane (40/60 v/v). BHTG was able to immobilize a variety of aqueous and organic solvents at concentration down to 1 mg/mL. In the mixed solvent, three-dimensional networks made up of helical ribbons form. The handedness of the ribbons depends on the rate of gel formation from hot solution. The formation of right-handed helical ribbons is kinetically favored, and that of left-handed helical ribbons is thermodynamically favored. A combination of spectroscopic, diffraction, and microscopic methods is used to approach the molecular ordering of BHTG in the gel and the formation and transition mechanism of chiral aggregates.

Results and Discussion

Synthesis. The gelator BHTG (Chart 1) was prepared via a multistep synthetic route (Scheme S1 in the Supporting Information). The glycosylation of 4'-hydroxy-4-bromobiphenyl with D-glucose pentaacetate, catalyzed by BF₃•OEt₂, led to 4'-bromobiphenyl- β -O-D-tetraacetylglucoside with good stereoselectivity.²⁸ The subsequent Suzuki cross-coupling reaction with 4-butoxyphenylboronic acid yielded 4'-butoxy-4-hydroxy-*p*-terphenyl- β -O-D-tetraacetylglucoside, which gave the target molecule after the deacetylation with freshly prepared CH₃ONa in the mixture of methanol and CHCl₃ (1/1 v/v). The target molecule and all of the intermediates were characterized by ¹H and ¹³C NMR, elementary analysis, and mass spectroscopy. All data agreed well with the expected structures. The presence of only one doublet with *J* = 7.3 Hz at δ = 4.91–4.94 ppm for the anomeric proton in the ¹H NMR spectrum of BHTG indicated a 100% β -glucosidic linkage (Figure S1).^{27a} The four small peaks in the 4.5–5.5 ppm region were ascribed to the hydroxyl protons of the sugar head,^{28b} which disappeared when D₂O was added to exchange out the protons (as evidenced in Figure S5). The specific optical rotation [α]₃₆₅ of BHTG was –34 (*c* = 10 mg/mL in DMF).

Gelation Test. To test the gelation ability of BHTG, a weighed amount of the sample and solvent were put into a septum-capped bottle and heated until all the solids dissolved. The solution was then allowed to cool in air (16 °C). Afterward, the bottle was inverted. If the mixture did not fall, it was recognized as a gel (Figure S2). Table 1 summarizes the testing results. BHTG gelled glycol, acetonitrile, acetic acid, 1,4-dioxane, tetrahydrofuran (THF), and toluene while dissolved in dimethyl sulfoxide (DMSO), dimethylformamide (DMF), and pyridine.

(27) (a) Shimizu, T.; Masuda, M. *J. Am. Chem. Soc.* **1997**, *119*, 2812–2818. (b) Shimizu, T.; Masuda, M.; Minamikawa, H. *Chem. Rev.* **2005**, *105*, 1401–1444.

(28) (a) Muller, H.; Tschierske, C. *J. Chem. Soc., Chem. Commun.* **1995**, 645–646. (b) Gridley, J. J.; Hacking, A. J.; Osborn, H. M. I.; Spackman, D. G. *Tetrahedron* **1998**, *54*, 14925–14946.

(17) (a) Hirst, A. R.; Smith, D. K. *Top. Curr. Chem.* **2005**, *256*, 237–273. (b) Hill, J. P.; Jin, W.; Kosaka, A.; Fukushima, T.; Ichihara, H.; Shimomura, T.; Ito, K.; Hashizume, T.; Ishii, N.; Aida, T. *Science* **2004**, *304*, 1481–1483. (c) Hanabusa, K.; Fukui, H.; Suzuki, M.; Shirai, H. *Langmuir* **2005**, *21*, 10383–10390. (d) Yoshida, M.; Koumura, N.; Misawa, Y.; Tamaoki, N.; Matsumoto, H.; Kawanami, H.; Kazaoui, S.; Minami, N. *J. Am. Chem. Soc.* **2007**, *129*, 11039–11041. (e) Huang, X.; Weiss, R. G. *Tetrahedron* **2007**, *7375*–7385. (f) Kundu, S. K.; Osaka, N.; Matsunaga, T.; Yoshida, M.; Shibayama, M. *J. Phys. Chem. B* **2008**, *112*, 16469–16477.

(18) Maeda, K.; Yashima, E. *Top. Curr. Chem.* **2006**, *265*, 47–88.

(19) Messmore, B. W.; Sukerkar, P. A.; Stupp, S. I. *J. Am. Chem. Soc.* **2005**, *127*, 7992–7993.

(20) (a) Thomas, B. N.; Corcoran, R. C.; Cotant, C. L.; Lindemann, C. M.; Kirsch, J. E.; Persichini, P. J. *J. Am. Chem. Soc.* **1998**, *120*, 12178–12186. (b) Thomas, B. N.; Lindemann, C. M.; Clark, N. A. *Phys. Rev. E* **1999**, *59*, 3040–3047.

(21) Zastavker, Y. V.; Asherie, N.; Lomakin, A.; Pande, J.; Donovan, J. M.; Schnur, J. M.; Benedek, G. B. *Proc. Natl. Acad. Sci. U.S.A.* **1999**, *96*, 7883–7887. (22) Lin, T.; Ho, R.; Sung, C.; Hsu, C. *Chem. Mater.* **2008**, *20*, 1404–1409.

(23) Lin, Y. C.; Kachar, B.; Weiss, R. G. *J. Am. Chem. Soc.* **1989**, *111*, 5542–5551.

(24) Furman, I.; Weiss, R. G. *Langmuir* **1993**, *9*, 2084–2088.

(25) Murata, K.; Aoki, M.; Suzuki, T.; Harada, T.; Kawabata, H.; Komri, T.; Olorseto, F.; Ueda, K.; Shinkai, S. *J. Am. Chem. Soc.* **1994**, *116*, 6664–6676.

(26) de Jong, J. J. D.; Lucas, L. N.; Kellogg, R. M.; van Esch, J. H.; Feringa, B. L. *Science* **2004**, *304*, 278–281.

Table 1. Gelation Experimental Results^a

solvent	H ₂ O	DMSO	DMF	pyridine	alcohol	acetone	ethyl acetate
state ^a	I	S	S	S	I	I	I
solvent	ethanediol	acetonitrile	acetic acid ^b	1,4-dioxane ^b	THF ^b	toluene	benzene
state ^a	G	G	G	G	G	G	I
appearance	O	T	O	O	T	T	/
$T_{\text{gel}}/^{\circ}\text{C}$	124	89	68	51	74	109	/
$C_{\text{gel}}/\text{mg/mL}$	4.2	2.7	6.4	9.5	8	1	/

^a Samples were prepared by fast-cooling procedure; concentrations = 5 mg/mL; G, gel; S, solubilization; I, insolubilization; T, translucent; some small crystallites or slightly opaque regions; O, opaque. ^b Measurement concentrations = 10 mg/mL. ^c T_{gel} : gel–sol transition temperature; the concentration is 10 mg/mL for acetic acid, THF, and 1,4-dioxane, while 5 mg/mL for other solvents. ^d C_{gel} : critical gelation concentration.

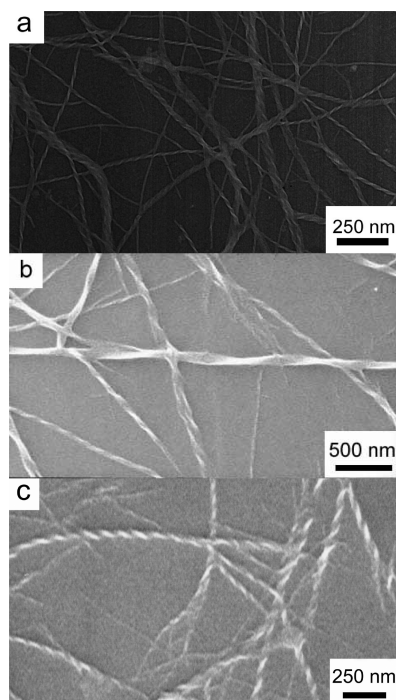


Figure 1. TEM picture of slow-cooled gel of BHTG (a), SEM images of the gels of BHTG obtained through slow-cooling process (b), and fast-cooling process (c). Solvent: H₂O/1,4-dioxane (40/60 v/v); concentration = 5 mg/mL.

Similar to its biphenyl analogues, 4-(4'-butoxyphenyl)phenyl- β -*O*-D-glucoside,^{15a} it was concluded that the self-assembly of BHTG was mainly driven by hydrogen bonding among sugar moieties, π - π stacking interaction among *p*-terphenyl segments, and hydrophobic interaction of butoxy tails. These interactions were so strong that the resultant gels were quite stable. For example, a gel of BHTG formed in glycol at a concentration of 30 mg/mL exhibits a very high gel–sol transition temperature (T_g) of 170 °C and was kept unchanged for more than 2 years at room temperature. The gelation experiments of BHTG in the mixture of H₂O/1,4-dioxane were carried out with two methods. “Fast-cooled gels” were obtained by allowing hot isotropic solution of BHTG to cool to room temperature (16 °C) immediately, while “slow-cooled gels” were obtained by putting the same hot isotropic solution into a water bath mediated with a PolyScience programmable temperature controller and allowed to cool from 70 °C to room temperature at a rate of 1 °C/min.

Electron Microscopy. Transmission electron microscopy (TEM) and scanning electron microscopy (SEM) were used to investigate the aggregate morphologies of BHTG in acetonitrile, toluene, 1,4-dioxane, and the mixture of 1,4-dioxane and water. Sheet aggregates were observed in the first solvent, while helical ribbons were found in the latter three (Figure S3 in the Supporting

Information), which reflected the influence of solvent nature on the suprastructure of BHTG in gels.^{15a} The morphology of the gel fiber in other solvents was not studied and was beyond the scope of the present work. One of the interesting morphological observations was that the handedness of the ribbons formed in 1,4-dioxane and its mixture with water depended on the rate of network formation. Figure 1a showed the TEM picture of BHTG network formed in the mixture of water and 1,4-dioxane (40/60 v/v), which consisted of helical ribbons with 20–150 nm diameters. Moreover, as demonstrated by SEM images, slow-cooled gels displayed left-handed helical ribbons (Figure 1b), while fast-cooled gel exhibited right-handed helical ribbons (Figure 1c). The pitch tilt was about 45° for the right-handed helices but about 60° for the left-handed ones. Similar results could be obtained at various concentrations (2–10 mg/mL) and compositions of mixed solvent of H₂O/1,4-dioxane (60/40–0/100 v/v) but were not obtained from other solvents. The reason is not known at the moment. In order to monitor the gelling process with UV–vis and circular dichroic spectroscopy, low critical gelation concentration (C_{gel}) was preferred. Therefore, the gelation behavior of BHTG was investigated in the mixture of H₂O and 1,4-dioxane at a fixed volume ratio of 40/60 in the subsequent study. The role of water addition was to reduce C_{gel} . The formation of right- and left-handed helical ribbons from enantiomerically pure BHTG suggested that the molecular chirality was not the only determining factor in helix formation of the present system.

Thomas, Clark, and co-workers have done a very nice work on the self-assembling of diacetylenic phospholipids.^{20b} Under differential phase contrast microscopy, they examined *in situ* the nucleation and growth of DC(8,9)PC at a very slow cooling rate from high enough temperature. It was found that roughly equal numbers of left- and right-handed helices were generated in the first seconds of tubule formation from spherical multilamellar vesicles of a pure enantiomer, followed by the formation of multilamellar tubules with single handedness exterior helical ridges. Unfortunately, the aggregates formed by BHTG are not as large as that of DC(8,9)PC and are not suitable for real-time optical microscopic observation. We therefore turn to other methods for help.

To exclude the possibility that the cooling rate causes the stereostructure variation of BHTG, Fourier transform infrared (FT-IR) and ¹H NMR spectroscopies were employed to characterize xerogels of both fast-cooled gels and slow-cooled gels. FT-IR is sensitive to the conformation of the glucoside group. For example, a typical peak around 890 cm⁻¹ originates from the vibration of C₁-H in β -form linkage, while the peak around 844 cm⁻¹ arises from that in α -form linkage.²⁹ The spectra of fast-cooled and slow-cooled xerogels were similar and both exhibited peaks at 896 cm⁻¹, implying that no β - to α -form configurational change occurred (Figure S4). In addition, the two samples showed

(29) Barker, S. A.; Bourne, E. J.; Whiffen, D. H. *Methods of Biochemical Analysis*; Interscience: New York, 1956; Vol. 3.

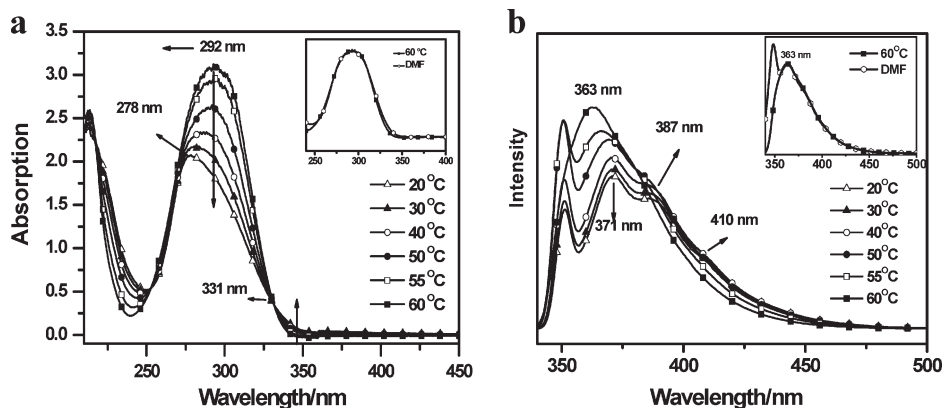


Figure 2. Temperature-variable absorption (a) and emission (b) spectra of BHTG in H₂O/1,4-dioxane (40/60 v/v) with a concentration of 2 mg/mL. The inset shows the absorption spectra of the sample at 60 °C and BHTG in DMF at 20 °C.

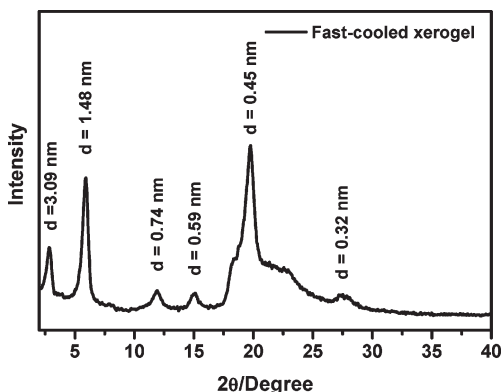


Figure 3. WAXD patterns of the xerogel obtained from the fast-cooled gel of BHTG in H₂O/1,4-dioxane and (40/60 v/v) at 5 mg/mL.

identical ¹H NMR spectra and equal specific optical rotations with the original gelator molecule, indicating again the chemical structure of gelator did not change during the gelling process.

Wet gels were also characterized in situ by ¹H NMR technique (Figure S5). However, the ¹H NMR spectra of BHTG recorded in D₂O/1,4-dioxane-*d*₆ (40/60 v/v) showed surprisingly little change between the dissolved state (65 °C) and the two gel states. The peaks in the gel samples might represent the fraction of molecules that were still dissolved at room temperature or in equilibrium with those adhered to the outside of gel fibers, while the signals from the molecules in the fibers became so broadened that they could no longer be observed. The increased area of the solvent peaks (water and 1,4-dioxane) relative to the gelator peaks in the gel samples seemed consistent with this speculation.

Spectroscopy. UV–vis and fluorescence spectroscopies were used to investigate the local ordering of BHTG in gel. Figure 2 shows the absorption and emission spectra of BHTG under various conditions. In the absorption spectra, BHTG shows a single broad structureless band with its maximum at 292 nm in DMF (a good solvent for BHTG). It was a typical absorption band of *p*-terphenyl and was assigned to ¹L_a.³⁰ In the fluorescence spectra, on the other hand, BHTG shows an emission peak at 363 nm along with a shoulder at 382 nm in DMF, which probably originated from the ring stretching vibration of *p*-terphenyl.^{30a} In the mixture of H₂O/1,4-dioxane (40/60 v/v) at 60 °C, BHTG

shows absorption and emission bands similar to that in DMF, suggesting that BHTG was molecularly dispersed in the mixed solvent at 60 °C. When the temperature was lowered to 20 °C, where the gel was generated, not only the maximal absorption blue shifts 14 nm but also the intensity around 340 nm enhances. It is known that *p*-terphenyl in the crystal state reveals the absorption of a low-lying ¹L_b state at around 340 nm, which is usually hidden or superimposed on the long-wavelength side of the strong ¹L_a band in solution.^{30b} Here, the increased intensity at 340 nm on the absorption spectra of BHTG suggested that the *p*-terphenyl of BHTG tended to take planar conformation in the aggregate state. Besides, the considerable blue shift indicated BHTG took an “H” type aggregate in gel.^{30a,31} Accordingly, red shifts in emission spectra were observed: at low temperature, the gel of BHTG exhibits a structured fluorescence with bands at 343, 371, 387, and 410 nm, while at 60 °C, only one peak centered at 363 nm was shown (Figure 2b). Fast-cooled sample gave similar results (Figure S6).

WAXD. The packings of BHTG in gels were further addressed by WAXD. Figure 3 shows the powder WAXD pattern of the fast-cooled xerogel of BHTG from H₂O/1,4-dioxane. There were three diffraction peaks corresponding to the *d* spacings of 3.09, 1.48, and 0.74 nm in the low-angle region. The *d* spacing ratio of 1:1/2:1/4 was consistent with a lamellar structure. The length of 3.09 nm was larger than the extended molecular length of BHTG (2.1 nm estimated by CPK molecular modeling) but smaller than twice the length suggesting an interdigitated bilayer structure with thickness of 3.1 nm. Similar result was observed for the slow-cooled xerogel (Figure S7).

Several models based on chiral elastic properties have been advised to depict the formation of self-assembled tubule and helical ribbons.³² It is believed that chiral molecules form bilayer membranes with some favored tilt, and therefore, the only way for molecules to twist with respect to their neighbors is for the entire membrane to twist. The favored tilt dictates a stable state, while the opposite direction is a metastable one. Increasing the temperature may have the effect to cause metastable- to stable-state transition as photoinduced conformation transition of the azo compound. In the interdigitated bilayer structure of BHTG, it was proposed that sugar heads were exposed outside and the *p*-terphenyl core and butoxy tail were shielded from water due to amphiphilic interactions, as shown in Scheme 1. It has been suggested in these models that the molecular tilt direction in the

(30) (a) Momicchioli, F.; Bruni, M. C.; Baraldi, I. *J. Phys. Chem.* **1972**, *76*, 3983–3990. (b) Dutta, A. K.; Misra, T. N.; Pal, A. J. *J. Phys. Chem.* **1994**, *98*, 12844–12848. (c) Geiger, H. C.; Perlstein, J.; Lachicotte, R. J.; Wyrozebski, K.; Whitten, D. G. *Langmuir* **1999**, *15*, 5606–5616.

(31) Kemnitz, K.; Tamai, N.; Yamazaki, I.; Nakashima, N.; Yoshihara, K. *J. Phys. Chem.* **1986**, *90*, 5094–5101.

(32) Selinger, J. V.; Spector, M. S.; Schnur, J. M. *J. Phys. Chem. B* **2001**, *105*, 7157–7169.

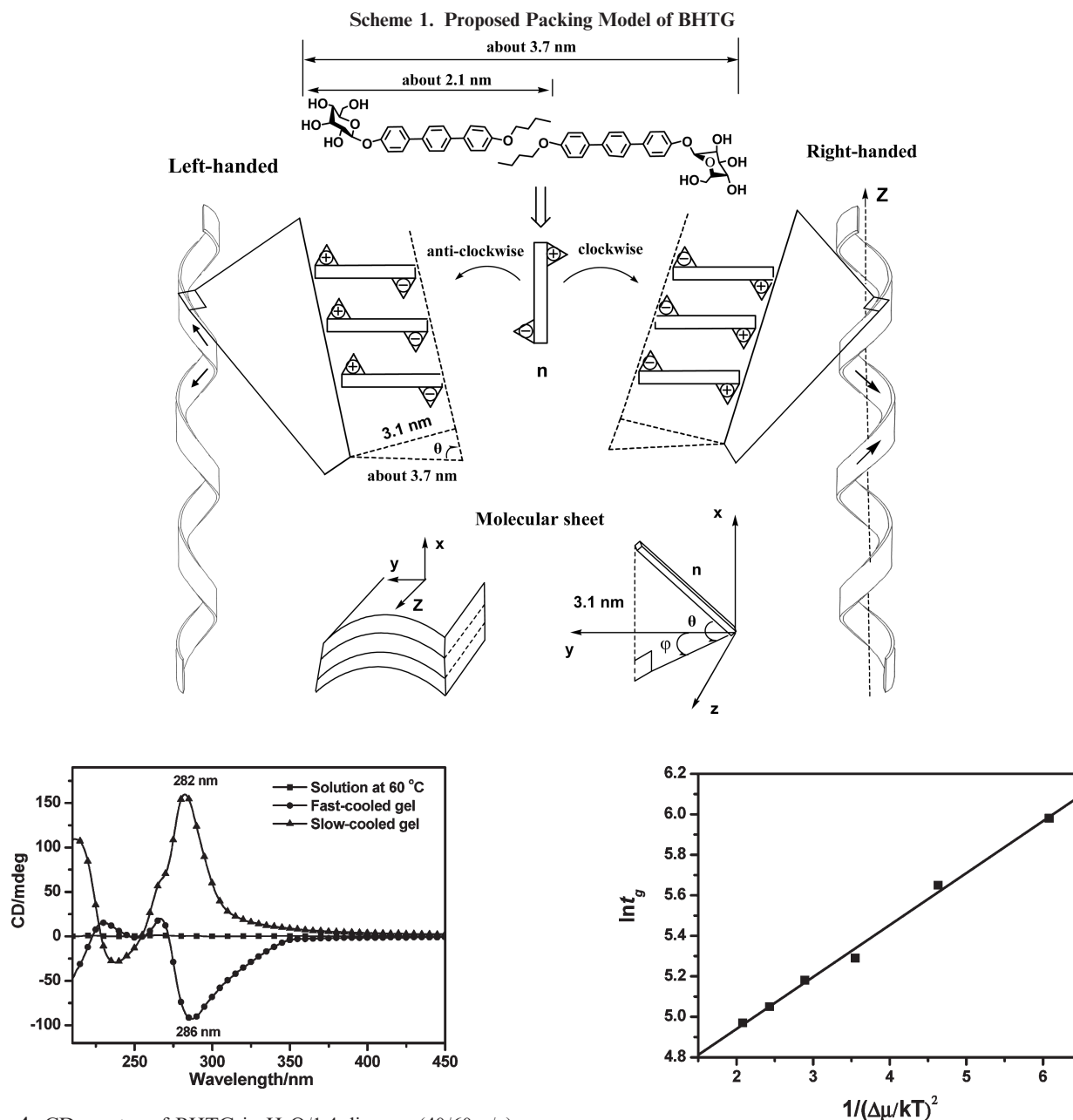


Figure 4. CD spectra of BHTG in H₂O/1,4-dioxane (40/60 v/v) with a concentration of 2 mg/mL in the solution state at 60 °C (■), fast-cooled gel state (●), and slow-cooled gel state (▲) at 20 °C.

bilayer membrane varied with molecular condensed phase: the molecular membranes with crystal structure have uniform tilt, while those with fluid structures (e.g., liquid crystal state) take various tilts.³² In the former case, the orientation of the molecular tilt is represented by the angle (φ) between the projection of the three-dimensional molecular director into the local tangent plane and the section of the ribbons and the local normal height.³³ Because the xerogels of BHTG from H₂O/1,4-dioxane exhibited sharp diffraction peaks, which indicated a crystal-like order, it was believed that BHTG arranged with a uniform tilt angle in bilayer membranes. Therefore, a possible molecular packing model was hypothesized, as shown in Scheme 1 in this file. The \mathbf{n} represents assembled dimer in the membrane, which was

Figure 5. The $\ln t_g - 1/(\Delta\mu/kT)^2$ plots for the mixture of BHTG in H₂O/1,4-dioxane (40/60 v/v).

depicted by two angles θ and φ . The θ depicted the tilt of \mathbf{n} , which could be estimated by the thickness of 3.1 nm (local normal height of one bilayer) and approximate length of dimer \mathbf{n} , and it was about 57° in both xerogels. The φ can be estimated by the pitch tilt of helical ribbons,³³ as mentioned above, 45° for right-handed ribbons and 60° for left-handed ribbons. Unfortunately, although the angles were reasonable in energy for these models, no more evidence can be obtained to further prove the accurate location. In the bilayer structure, the dimer can tilt with two different orientations: clockwise and anticlockwise, which was considered to clarify the opposite helical ribbons. However, the exact relationship between molecular orientation and supramolecular helicity was unclear.

Tuning the Helicity. The helical ribbons with opposite sense in the microscopic images of fast- and slow-cooled gels illustrated chiral structures at the fiber levels. In order to probe the chiral

(33) (a) Helfrich, W.; Prost, J. *Phys. Rev. A* **1988**, *38*, 3065–3068. (b) Ou-Yang, Z. C.; Liu, J. X. *Phys. Rev. A* **1991**, *43*, 6826–6836. (c) Chung, D. S.; Benedek, G. B.; Konikoff, F. M.; Donovan, J. M. *Proc. Natl. Acad. Sci. U.S.A.* **1993**, *90*, 11341–11345.

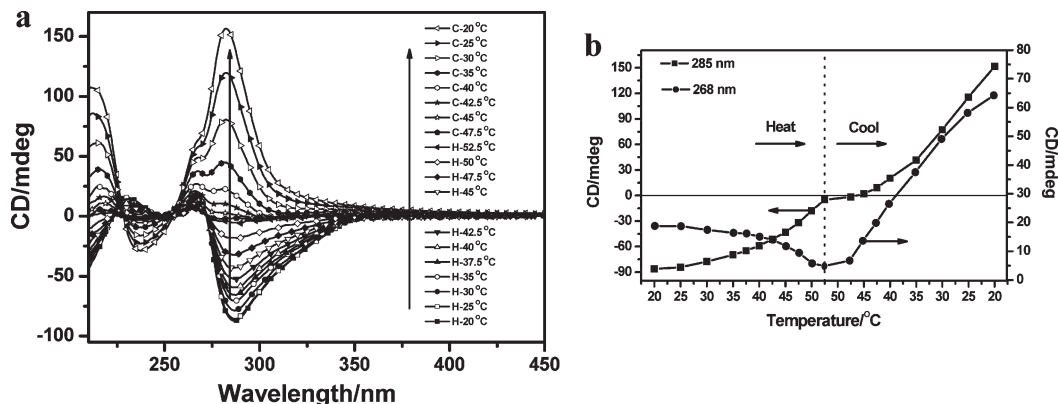


Figure 6. Temperature-variable CD spectra of the gel of BHTG in $\text{H}_2\text{O}/1,4\text{-dioxane}$ (40/60 v/v) at 2 mg/mL (a) and the variety of the peak of the band centered at 285 (■) and 268 (●) nm.

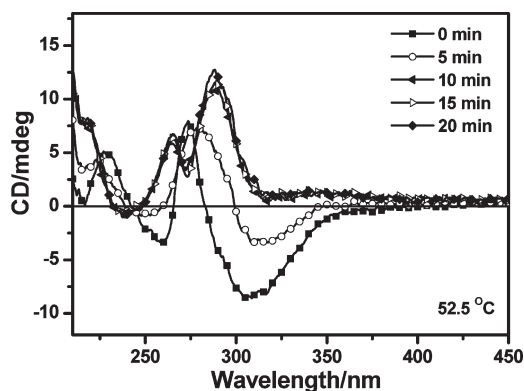


Figure 7. Time-variable CD spectra of the gel of BHTG in $\text{H}_2\text{O}/1,4\text{-dioxane}$ (40/60 v/v) at 52.5 °C with a concentration of 2 mg/mL.

packing at the molecular level, CD spectroscopy, which is extremely sensitive to the intermolecular chiral order at the molecular level,⁶ was used. Figure 4 shows the CD spectra of BHTG in $\text{H}_2\text{O}/1,4\text{-dioxane}$ at different conditions. At 60 °C, where molecules were dispersive, the mixture exhibits negligible CD effect. With decreasing the temperature of the mixture, the resultant gels show intense CD effect in the absorption region of *p*-terphenyl, suggesting the formation of chiral self-assemblies. The fast-cooled gel shows an intensive negative CD band at 286 nm and two small positive bands centered at 266 and 230 nm, while the slow-cooled gel exhibits a positive band centered at 214 nm, a negative band centered at 236 nm, and a intensive positive band centered at 282 nm along with a shoulder band centered at 264 nm. The opposite CD effect paralleled the helicity of the ribbons obtained from different cooling rate, implying that the reversed helicity of the ribbons resulted from the different molecular orientation at the molecular level.

In chiral or biased chiral symmetry-breaking theory, which develops from these models mentioned above,^{32,34} it is suggested that the chirality of the membrane contributes to a collective tilt of the molecules with respect to the membrane normal rather than chiral intermolecular interaction. Within the framework of chiral symmetry-breaking theory, chiral aggregates may result even from achiral molecules.^{17b,35} The theories have been successfully used to explain diacetylenic phospholipid systems where minority handedness was observed during the kinetic process of tubule formation at high lipid concentration.²⁰ This is an important

concept that the diacetylene group in the long tail acts as a kink to cause the rod-like molecules to pack stably with P-twist or M-twist orientation.³² Here the *p*-terphenyl segments which exhibited strong π - π interaction are similar to the diacetylene group in the nature of packing kink action. It had been mentioned above that in the interdigitated bilayer structure BHTG can break into two packing orientations: clockwise and anticlockwise, as show in Scheme 1. The opposite orientation of molecular packing was considered to clarify the different helical sense. However, on the principle of biased chiral symmetry-breaking theory,³⁴ the stabilities of the two molecular tilted orientations were different due to the chirality of the glycosyl part: one was stable, while another was metastable.

The formation of crystal fibers of BHTG was essentially controlled by a kinetic nucleation–growth process.³⁶ The nucleation process can be verified by the linear relationship between $\ln t_g$ and $1/(\Delta\mu/kT)^2$ (t_g is the induction time of nucleation, $\Delta\mu$ denotes the chemical potential difference between BHTG molecules in the fiber and in the liquid phase, k is Boltzmann's constant, T is temperature; the equations used to get the relationship are shown in Supporting Information). Because the absorption bands of BHTG and its aggregates were far away from 500 nm, the transparency at 500 nm was used to monitor the self-assembled process. The values of t_g with various concentrations were recorded (Figure S8), and the relationship of $\ln t_g$ and $1/(\Delta\mu/kT)^2$ is shown in Figure 5. The $\ln t_g$ increased linearly with $1/(\Delta\mu/kT)^2$, indicating that the self-assembly of BHTG in $\text{H}_2\text{O}/1,4\text{-dioxane}$ was a nucleation–growth process.

CD spectroscopy was used to investigate the evolution of supramolecular chirality in the nucleation–growth process. The process of BHTG in $\text{H}_2\text{O}/1,4\text{-dioxane}$ (40/60 v/v) from 60 to 20 °C with a cooling rate of 1 °C/min was monitored via CD spectroscopy (Figure S9). At 37.5 °C, the mixture exhibited a negative band at 305 nm and a positive band at 280 nm. The two bands intersected the abscissa at 292 nm, the position of absorption maximum, indicating the appearance of chiral molecular clusters. When the temperature decreased to 35 °C, the negative band disappeared and was replaced by a positive band centered at 294 nm. The M–P transition suggested that, during the slow-cooling process, metastable molecular clusters (“nuclei”) formed at first and then transferred into the stable state.

Because of the high degree of supersaturation of the solution during nucleation, the appearance of the transition from metastable

(34) Seifert, U.; Shillcock, J.; Nelson, P. *Phys. Rev. Lett.* **1996**, *77*, 5237–5240.

(35) Ribo, J. M.; Crusats, J.; Sagues, F.; Claret, J.; Rubires, R. *Science* **2001**, *292*, 2063–2066.

(36) (a) Liu, X. Y. *Langmuir* **2000**, *16*, 7337–734. (b) Liu, X. Y.; Sawant, P. D.; Tan, W. B.; Noor, I. B. M.; Pramesti, C.; Chen, B. H. *J. Am. Chem. Soc.* **2002**, *124*, 15055–15063.

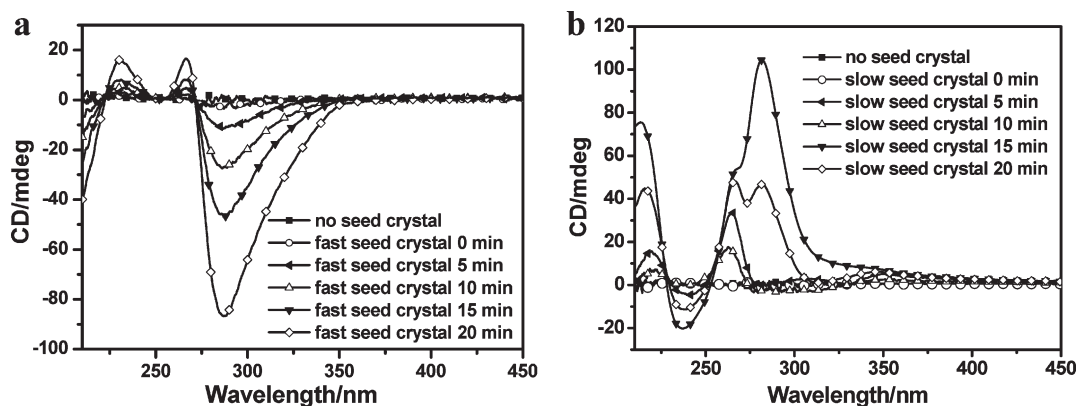


Figure 8. Time-variable CD spectra of BHTG in H₂O/1,4-dioxane (40/60 v/v) at 40 °C with a concentration of 2 mg/mL after injecting 1 wt % fast-cooled (a) or slow-cooled (b) gel of BHTG in H₂O/1,4-dioxane (40/60 v/v) with a concentration of 2 mg/mL as seed crystal. The gels as seed crystal were located in a water bath of 40 °C before injection.

to stable state was transitory and, therefore, it was difficult to further investigate their properties in the cooling process. In contrast, in the heating process, it was possible to get the metastable state longer via subtly controlling temperature. Figure 6a shows the CD spectra of the fast-cooled gels of BHTG in H₂O/1,4-dioxane (40/60 v/v) at 2 mg/mL during a heating–cooling process. It was found that the transition of a negative CD signal to a positive one appeared at 52.5 °C as the fast-cooled gel did not dissolve completely (generally, if the fast-cooled sample with negative CD signals was heated to dissolve completely and then cooled slowly, they always exhibit positive CD signals, as that in Figure 4, but the CD signal disappeared when gel dissolved completely). The intensities of CD spectra at 285 and 268 nm at different temperature are plotted with temperature as abscissa to track the transition, as shown in Figure 6b. Though the signal at 285 nm exhibits M–P transition while that at 268 nm does not, the signals at 285 and 268 nm both show a transition region of 50–52.5–50 °C (heated and then cooled process). The M–P transition of the CD signal suggested that molecules modulated stacking orientation from the metastable state to the stable one in this temperature region. To further confirm this proposal, the fast-cooled gel was directly annealed at 52.5 °C, as that shown in Figure 7. When heated to 52.5 °C, the fast-cooled gel exhibits a negative band centered at 305 nm at first. With increasing annealing time, the band became small and turned to be a positive band centered at 293 nm, which was stable for further annealing, indicating the formation of the thermodynamically controlled molecular cluster of BHTG (when annealed gel was heated to dissolve completely and then cooled rapidly to 20 °C, a negative CD signal appeared again). Furthermore, the M–P transition did not occur when the fast-cooled gel was annealed at 47.5 °C (Figure S10), suggesting that molecular nucleation and rearrangement occurred in the region of 50–52.5–50 °C. Consequently, the molecular clusters with opposite molecular arrangements could be obtained by subtly controlling temperature, supplying the possibility to probe the chiral inducing ability of nuclei to grown-up fibers.

At first, the fast-cooled sample, which had remained at 47.5 °C for 30 min, was cooled to room temperature slowly (Figure S10). The resultant gel reveals negative Cotton effect at 290 nm, contrary to the positive Cotton effect of slow-cooled gel (Figure 4). The opposite sense of two gels obtained from the slow-cooling process indicated that the helix of ribbons was determined in nucleation. On the other hand, when the fast-cooled sample had remained at 52.5 °C for a long enough time for M–P

transition, positive CD signals were observed regardless of the cooling rates. These results further confirmed the inducing ability of the molecular cluster acted as nuclei to the supramolecular chirality.

On the basis of the results above, the self-assembling mechanism and process of BHTG with cooling rate dependence of supramolecular chirality was hypothesized. At first, BHTG was dispersed in the solution at high temperatures. With decreasing temperature, molecules self-assembled into clusters as nuclei. The nuclei with metastable supermolecular chirality formed at first, and they would evolve into stable ones as annealed at the temperature of nucleation for a time long enough. In the fast-cooling process, the metastable nuclei would directly grow up to right-handed ribbons, while in the slow-cooling process, the metastable nuclei evolved into stable nuclei and then further aggregated to be left-handed ribbons. In the gel state, the right-handed ribbons could not evolve to the left-handed ribbons due to the kinetically controlling network structures. Consequently, the right-handed ribbons were obtained via kinetically controlling process, while left-handed ribbons were obtained via a thermodynamically controlling process.

Under the framework of the mechanism above, it was expected that, in a supersaturation solution of BHTG in H₂O/1,4-dioxane, well-defined chiral ribbons would be obtained by adding prepared fast-cooled or slow-cooled gel as “seed crystal”. It was known that, when cooled slowly from the solution phase, the mixture of BHTG in H₂O/1,4-dioxane (40/60 v/v) at a concentration of 2 mg/mL did not gelate until the temperature of the mixture fell to 37.5 °C, while the M–P transition occurred at a temperature higher than 47.5 °C (Figure S9 in the Supporting Information and Figure 7). On the other hand, the supersaturated solution of BHTG in H₂O/1,4-dioxane (40/60 v/v) at a concentration of 2 mg/mL did not gel at 40 °C even for more than 1 h (the result was not shown), and therefore, it was a good candidate to probe the inducing ability of added “seed crystal”. The fast-cooled and slow-cooled gels were prepared beforehand as “seed crystal” and were located in a water bath of 40 °C before being injected into the supersaturated solution. Figure 8 shows the CD spectra of BHTG in H₂O/1,4-dioxane (40/60 v/v) at a concentration of 2 mg/mL at 40 °C after 1 wt% gel as seed crystal was injected. The solution containing the seed crystal at 0 min exhibits no discernible CD signals due to the small amount of seed crystal. As expected, with increasing growth time, the mixture containing fast seed crystal shows negative CD signals as that of fast-cooled gel, while the mixture containing slow seed crystal shows positive signals as that of slow-cooled gel. The opposite CD signals of supersaturated

solutions containing seed crystals prepared via different cooled rates showed that the supramolecular chirality of added gel determined the helical senses of ribbons in the gels obtained from supersaturated solutions.

Conclusion

A new LMMG, BHTG, was synthesized and employed to efficiently immobilize a variety of solvents. In the mixture of H₂O and 1,4-dioxane, three-dimensional networks made up of helical ribbons were generated. The handedness of helical ribbons could be mediated by the rate of gelation: the fast-cooling process yielded right-handed helical ribbons, while the slow-cooling process yielded left-handed counterparts. Microscopic, spectroscopic, and diffraction analyses suggested that BHTG aggregated into a twisted interdigitated bilayer structure with a thickness of 3.1 nm through a kinetically controlled nucleation–growth process. After being cooled from the hot solution, the molecularly dispersed BHTG self-assembled to form chiral associates, which acted as nuclei for the ribbons to grow. The molecules of BHTG had two kinds of arrangements in the nuclei, clockwise and anticlockwise orientations. One was metastable and was formed at high temperature immediately after the self-assembly of BHTG occurred and gradually transformed into the stable one with decreasing temperature. Fast-cooling process did not leave enough time for the nuclei to evolve from the metastable to the stable state. As a result, the ribbons grown from the metastable nuclei had right handedness. During slow-cooling process, however, the metastable nuclei transformed into the stable one and dictated the molecules of BHTG to pack in a left-handed way. Such a method has been used to tune the helicities of twisting ribbons generated by the analogues of BHTG, that is, 4-(4'-

alkoxyphenyl)phenyl- β -*O*-D-glucoside ($n = 1-12$), in the mixture of water and 1,4-dioxane.³⁷ Among them, 4-(4'-pentyloxyphenyl)phenyl- β -*O*-D-glucoside and 4-(4'-hexyloxyphenyl)phenyl- β -*O*-D-glucoside were found to show obvious cooling-rate-dependent supramolecular chirality. Therefore, this work provides a convenient way to tune the chirality of supramolecular structure for some gelators with delicately designed structures. We will introduce vinyl group(s) to the molecule of BHTG and try to stabilize the resultant chiral aggregates by polymerization or cross-linking, targeting for the novel chiral template of nanomaterials and the chiral carrier of asymmetric catalysts.

Acknowledgment. We thank the National Natural Science Foundation of China through the General Program (No. 20674001), Key Program (No. 20834001), and the National Science Fund for Distinguished Young Scholars (No. 20325415) for the financial support.

Note Added after ASAP Publication. This article was published ASAP on November 18, 2009. Reference 13(f) has been modified. The correct version was published on December 1, 2009.

Supporting Information Available: Synthesis and characterization of BHTG, gel pictures, FT-IR spectra of BHTG and UV–vis and fluorescence spectra of **1** in H₂O and 1,4-dioxane, and turbidity measurement for nucleation process and the equations of dynamic calculation. This material is available free of charge via the Internet at <http://pubs.acs.org>.

(37) Details will be reported.